Optics and Lasers in Engineering 84 (2016) 44–50

Contents lists available at ScienceDirect

Optics and Lasers in Engineering

journal homepage: www.elsevier.com/locate/optlaseng

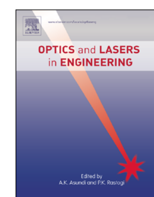

Ablation depth control with 40 nm resolution on ITO thin films using a square, flat top beam shaped femtosecond NIR laser

Hoon-Young Kim [a,b], Ji-Wook Yoon [a,b], Won-Suk Choi [a,b], Kwang-Ryul Kim [c], Sung-Hak Cho [a,b,*]

[a] Nano Machining Laboratory, Korea Institute of Machinery & Material (KIMM), 171 Jang-dong, Yuseong-gu, Daejeon 305-343, South Korea
[b] Department of Nano-Mechatronics, Korea University of Science & Technology (UST), 176 Gajung-dong, Yuseong-gu, Daejeon 305-343, South Korea
[c] Department of Electronic and Electrical Engineering, SungKyunKwan University, 300 Chunchun-dong, Jangan-gu, Suwon 440-746, South Korea

ARTICLE INFO

Article history:
Received 30 June 2015
Received in revised form
23 January 2016
Accepted 25 March 2016

Keywords:
Ablation depth control
Femtosecond laser
Indium tin oxide (ITO)
Beam shaping
Transparent conducting electrode

ABSTRACT

We reported on the ablation depth control with a resolution of 40 nm on indium tin oxide (ITO) thin film using a square beam shaped femtosecond (190 fs) laser ($\lambda_p = 1030$ nm). A slit is used to make the square, flat top beam shaped from the Gaussian spatial profile of the femtosecond laser. An ablation depth of 40 nm was obtained using the single pulse irradiation at a peak intensity of 2.8 TW/cm^2. The morphologies of the ablated area were characterized using an optical microscope, atomic force microscope (AFM), and energy dispersive X-ray spectroscopy (EDS). Ablations with square and rectangular types with various sizes were demonstrated on ITO thin film using slits with varying *x*–*y* axes. The stereo structure of the ablation with the depth resolution of approximately 40 nm was also fabricated successfully using the irradiation of single pulses with different shaped sizes of femtosecond laser.

© 2016 Published by Elsevier Ltd.

1. Introduction

Indium tin oxide (ITO) is widely used as a transparent conducting electrode for the fabrication of optoelectronic products such as flat panel displays, touch panels, solar cells, and organic light-emitting devices (OLEDs) due to its high electrical conductivity and high transmittance in the visible and near infrared (NIR) wavelength range [1]. In the field of display fabrication and assembly, methods of controlling the micromachining depth of the ITO thin films deposited on substrates as glass or Polyethylene terephthalate (PET) were crucial for enhancing the optical transmittance in order to reduce the power consumption and for improving the electrical conductivity of ITO thin films in order to reduce the resistance [2]. Although methods of patterning the ITO thin film structure are predominantly surface monolithic processing techniques such as photolithography [3], there have been technical issues in patterning on ITO thin films in the terms of complexity, speed, and cost; the patterning also requires sophisticated facilities and costly equipment as well as environment-unfriendly toxic chemicals [4]. If direct patterning on ITO thin films with depth controlled and well defined morphologies can be accomplished easily, it could be used at a low cost in various applications such as OLED displays, flat panel displays, touch panels, solar cells, smartphones, and various electronic devices [5].

The interactions between ultrashort, high-intensity lasers and several materials have become significant areas of interest since the advent of high-intensity femtosecond lasers. Laser ablation is the technology to remove target material from the substrate through absorbing the laser energy, which can achieve the desired area of clean patterning due to the local heating and material removal [6]. In general, ultrashort pulse lasers induce small thermal defects in the material compared with the irradiation of long pulse lasers [7]. Above all, femtosecond lasers induce a precise ablation threshold with reduced laser fluence due to their high peak intensity with low pulse energies via the ultrashort pulse duration. These attractive characteristics of femtosecond lasers have stimulated the flexibility of laser micro-machining and minimized thermal defects such as micro-cracks and debris. Thus, femtosecond lasers have been used as accurate material removal tools in optoelectronic product fabrications due to their minimized thermal effects on the materials [8]. Recently, significant attention has focused on making the control of the ablation depth on ITO thin films become more efficient, particularly for transparent electrodes in high-density optoelectronic devices [9]. Although several experiments of laser ablation on ITO thin films have been reported

* Corresponding author at: Nano Machining Laboratory, Korea Institute of Machinery & Material (KIMM), 171 Jang-dong, Yuseong-gu, Daejeon, 305-343, South Korea. Tel.: +82 42 868 7077.
E-mail address: shcho@kimm.re.kr (S.-H. Cho).

http://dx.doi.org/10.1016/j.optlaseng.2016.03.025
0143-8166/© 2016 Published by Elsevier Ltd.

[10–12], the depth controls of the ablation area have not yet been studied in detail, primarily because laser beams with circular Gaussian spatial profiles have typically been used in previous studies [13,14]. Gaussian beams have significantly different spatial intensity profiles between the center and edge of the focused beam. Recently, some research groups have reported laser ablation on ITO thin films using several beam shaping techniques that were applied to solar cells [15,16] and electrical devices [9]. However, experimental results have not yet been reported for well-defined, square-shaped ablation structures on ITO thin films with the depth control of several tens of nanometers using the NIR femtosecond laser.

In this paper, we reported on the ablation depth control with a resolution of 40 nm on indium tin oxide (ITO) thin films through controlling the pulse numbers of the femtosecond (190 fs) laser ($\lambda_p = 1030$ nm) with a square beam. The beam that was shaped to have a flat top from a Gaussian beam passed through a slit was applied to the femtosecond laser patterning of ITO films. The morphologies of the ablated areas were characterized using an optical microscope, atomic force microscope (AFM), and energy dispersive X-ray spectroscopy (EDS). Square and rectangular ablations with different sizes were fabricated on ITO thin films using a slit with varying *x*–*y* axes. The stereo structure of the ablation with a depth resolution of approximately 40 nm was also demonstrated through controlling a single pulse with varying sizes of the square beam shaped femtosecond laser. Although femtosecond laser ablations on ITO thin films have been investigated previously, to the best of our knowledge, this is the first report of the ablation depth control with a 40 nm resolution. This process might be a useful tool for high precision machining on ITO thin films in electronic devices and display components using high-intensity femtosecond lasers.

2. Experimental

The experimental setup was presented in Fig. 1. In the experiments, a commercial regenerative amplified mode-locked Yb:KGW laser (Model no.: S-Pulse HR, Amplitude Systemes, France) with a central wavelength of 1030 nm, a pulse duration of 190 fs, a repetition rate of 30 kHz, and a maximum pulse energy of 66 uJ was used. The pulse energy was measured using a power meter. The beam had a diameter of 3 mm and the M^2 quality parameter was 1.2. The laser beam was focused using an objective lens with 0.42 NA (Model no.: M Plan Apo NIR 50x, Mitutoyo). The laser beam was focused at the front of the sample in order to avoid direct ablation on the ITO by the lens. Then, the propagating defocused, shaped laser beam was irradiated via the slit onto the surface of the ITO thin film as depicted in Fig. 1(b). The ITO thin film sample was fixed on a micro positioning stage controlled by a computer, and it could be moved in the directions of *x*-, *y*-, and *z*-axes. The pulse energy of laser was controlled using neutral density filters. The femtosecond laser beam had linear polarization and the beam profile of spatial Gaussian. As seen in Fig. 1, the Gaussian beam was shaped via the slit in order to have a flat top. The flat top beam had a square shape due to the slit control. In this study, the following laser ablation experiments were conducted in order to control the ablation depth of the ITO thin film on the glass substrate using the shaped flat top beam and to accomplish selective removal between the ITO thin film and glass substrate.

Information regarding the sample was presented in Fig. 2. ITO thin films with a nominal thickness of 150 nm and a transmittance of 90.5% (In_2O_3:SnO_2=90:10) were deposited on the glass substrates (20 × 20 × 1.1 mm) using a DC magnetron sputtering system. The six sides of the glass substrate were optically polished. The sheet resistance of 10–15 Ω was used in the experiments. The ITO thin film was a commercial sample provided by WOOYANG GMS Korea (www.solaronix.co.kr).

The surface characteristics of the ablated ITO thin films were observed using an optical microscope (MM-20, Nikon), and the three-dimensional data and cross-section samples perpendicular to the ablated ITO thin film patterns were prepared using a scanning probe microscope (XE-100, Park Systems). Finally, the energy dispersive spectroscopy (Shrion, FEI) was used to identify the remained elements at the selective ablation area between the ITO thin film and glass substrate.

3. Results and discussion

In this study, experiments were conducted to control a single pulse using the flat top beam shaped by a slit in order to control the ablation depth. The well-defined localization of the photon energy is crucial for removing the thin layers from the substrate

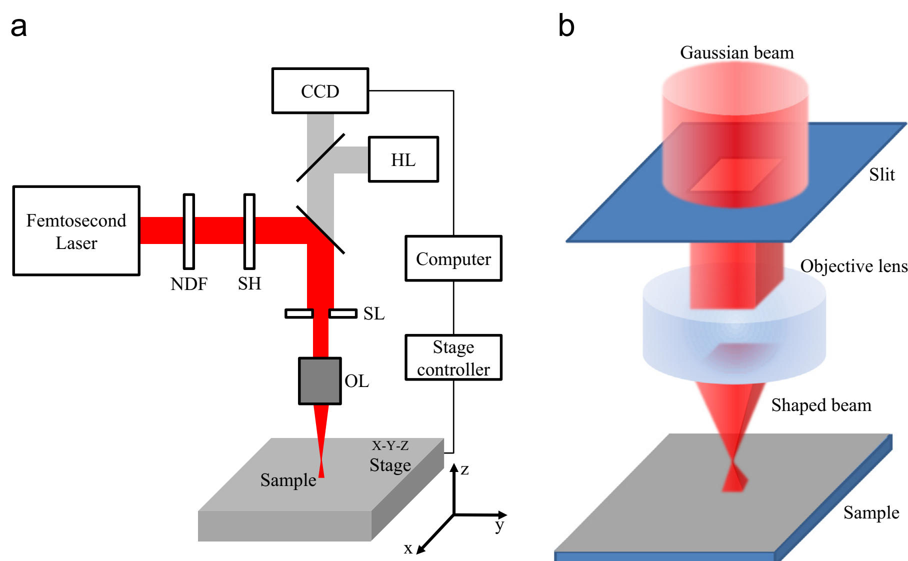

Fig. 1. (a) Schematical representation of the femtosecond laser system with a slit used in the experiment (NDF: Neutral density filter, SH: Shutter, HL: Halogen lamp, SL: Slit, OL: Objective lens). (b) Basic concept of the shaped beam using the slit.

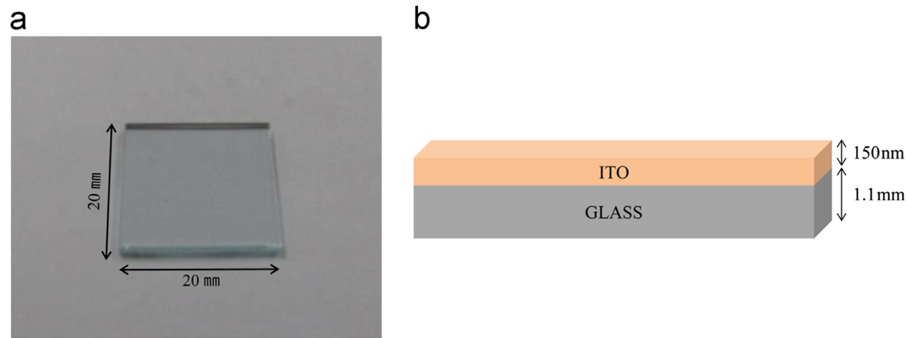

Fig. 2. Photograph of the (a) sample and (b) sample information.

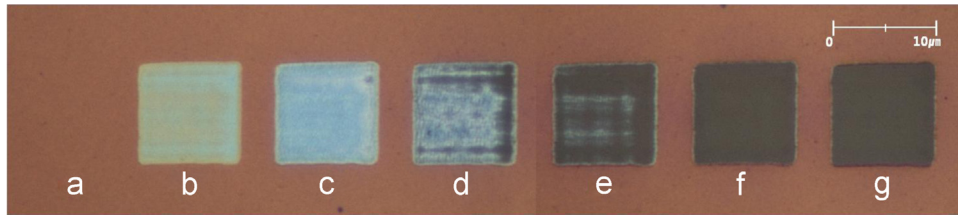

Fig. 3. Optical microscopic views of the morphology of the ablated ITO film using IR femtosecond laser irradiation with different pulse shots: (a) 0 shots, (b) 1 shot, (c) 2 shots, (d) 3 shots, (e) 4 shots, (f) 5 shots, and (g) 6 shots. The irradiated intensity of the laser beam was 2.8 TW/cm^2.

with minimized thermal effects for ultrafast laser ablation of any material. The material removal only occurs if the pulse energy reaches an ablation threshold, which is strongly dependent on the material characteristics. For multilayer substrates, the ablation threshold for each layer is the most important controlling factor for the selective removal of the desired layer. The ablation threshold of the ITO thin films and glass substrates were measured in order to avoid damage on the glass substrate and to conduct selective ablation successfully. The measured ablation threshold of the ITO thin films in this experiment was 0.14 J/cm^2 with a 190 fs pulse duration. Ashkenasi et al. reported that the ablation threshold of ITO thin films was approximately 0.2 J/cm^2 with a pulse width of 200 fs [17]. The difference in these thresholds could be explained by the different etching rate due to the distinct nature of each ITO thin film or the discrepancy of the exact pulse shape of the ultrafast laser used in the ablation experiment. The measured damage threshold of the glass substrate was 2.2 J/cm^2 at 190 fs in the experiment. Selective ablation of the ITO layer without damage to the glass substrate was realized at the laser fluence between the ablation threshold of the ITO thin film and glass substrate.

The optical microscope images of the morphology on the ablated ITO thin film at the pulse irradiation for 1–6 shots were presented in Fig. 3. The fluence of the irradiation laser was fixed at 0.8 J/cm^2 in order to investigate the depth control on the ITO thin film in the experiment. The fluence was higher than the ablation threshold of ITO thin film (0.14 J/cm^2) and less than that of glass substrate (2.2 J/cm^2). The peak power density was calculated about 2.8 TW/cm^2 on the input surface of the ITO thin film when a 0.8 J/cm^2 beam was irradiated. The ablated area was observed using a microscope with a CCD camera and it was recorded on a computer. A square pattern with a size of 10 × 10 μm was fabricated using the slit's size control. No change was observed when the laser pulse was not irradiated (Fig. 3(a)). However, the ablation was first observed after a single laser pulse irradiation at peak intensity of 2.8 TW/cm^2 (Fig. 3(b)). Ablations were observed after increasing the number of laser pulse irradiations (Fig. 3(c) to (g)). When six laser pulses were irradiated on the ITO thin film, it was fully ablated and removed from the glass substrate. A different color was exhibited in each ablated area. It was observed that the color become darker as the number of irradiated laser pulses increased. Therefore, it was inferred that the selective ablation between the ITO layer and glass substrate was successfully achieved after the irradiation of six laser pulses.

The three-dimensional morphologies of the cross-sectional profile with each different pulse shot were presented in Fig. 4. The morphology of the ablated area was measured using an atomic force microscopy (AFM). The 3D morphology in Fig. 4(a) was the same as that of Fig. 3(b). Fig. 4(b)–(f) align with Fig. 3(c)–(g). As discussed regarding Fig. 3, the ablation depth on the ITO thin film increased when the irradiated pulses increased.

The measured two-dimensional depth morphologies of the cross-section in the ablated area were presented in Fig. 5. It was measured that the average depths of the square shaped ablation were approximately 40 ± 3 nm (Fig. 5(a)), 80 ± 5 nm (Fig. 5(b)), 110 ± 6 nm (Fig. 5(c)), 130 ± 8 nm (Fig. 5(d)), 140 ± 11 nm (Fig. 5(e)), and 150 ± 15 nm (Fig. 5(f)). The 2D depth morphology in Fig. 5(a) was the same as the sample in Fig. 3(b) and Fig. 4(a). Fig. 5(b)–(f) align with Fig. 3(c)–(g). It was found that the minimum resolution of the controllable ablation depth was 40 nm on the ITO thin film using the square-shaped beam femtosecond laser. The definition of the 40 nm resolution is the average of the ablated depth rate at one pulse irradiation. The Rayleigh length was 10.7 μm. It was considered that different ablated depth rates were induced by the different peak intensities at the irradiated focal spots. This indicated that the ablated spot on the surface of the ITO thin film that resulted from the tightly focused propagating femtosecond laser pulse changed slightly according to the z-axis direction due to the increase in the irradiated laser pulses. For the pulse shots from 1 to 6, the ablation depth was ranged from 40 to 150 nm with an immovable ablation width of 10 μm. Because there were increasing pulse shots from the laser, the ablation depth increased, as depicted in Fig. 5. From the measured cross-sectional profile of the ablated ITO thin film, it was clarified that the controllable depth of ablated pattern by single pulse irradiation was approximately 40 nm as seen in Fig. 5(a). Furthermore, it was observed that the ITO thin film layer was completely removed without damage to the glass after the irradiation of six pulses

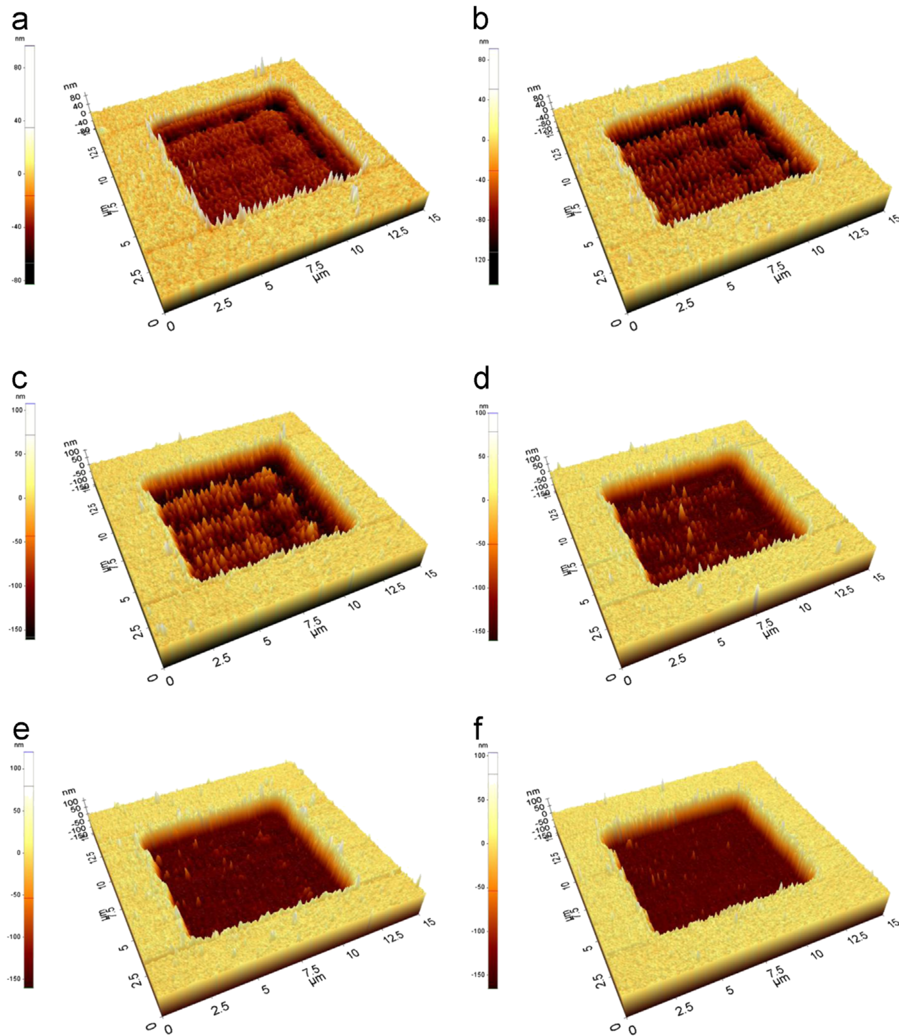

Fig. 4. Images of the AFM 3D morphology data using IR femtosecond laser irradiation with different pulse shots: (a) 1 shot, (b) 2 shots, (c) 3 shots, (d) 4 shots, (e) 5 shots, and (f) 6 shots.

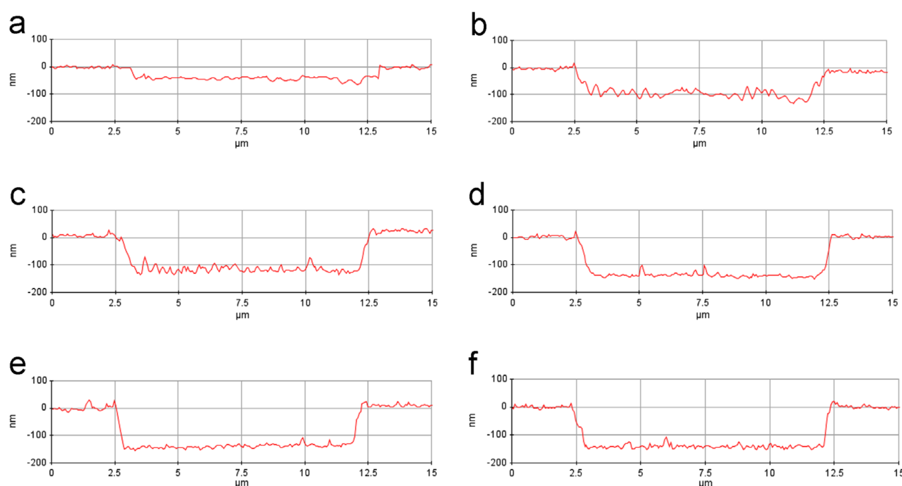

Fig. 5. The AFM cross-sectional graph using the IR femtosecond laser irradiation with different pulse shots: (a) 1 shot, (b) 2 shots, (c) 3 shots, (d) 4 shots, (e) 5 shots, and (f) 6 shots.

(Fig. 5(f)). There were ridges on both sides of the ablations; the ridge heights at the boundary of the ablated area were less than 10 nm (Fig. 5(a) to (f)). For the strategy to get the finest depth control, one way is to use single fs pulse with the energy fluence or intensity just above the ablation threshold, the other way is to use a low energy/intensity fs pulse with the control of repetition rate (up to MHz) and shot number. The relationship between single shots with high energy fluence and high repetition rate with low

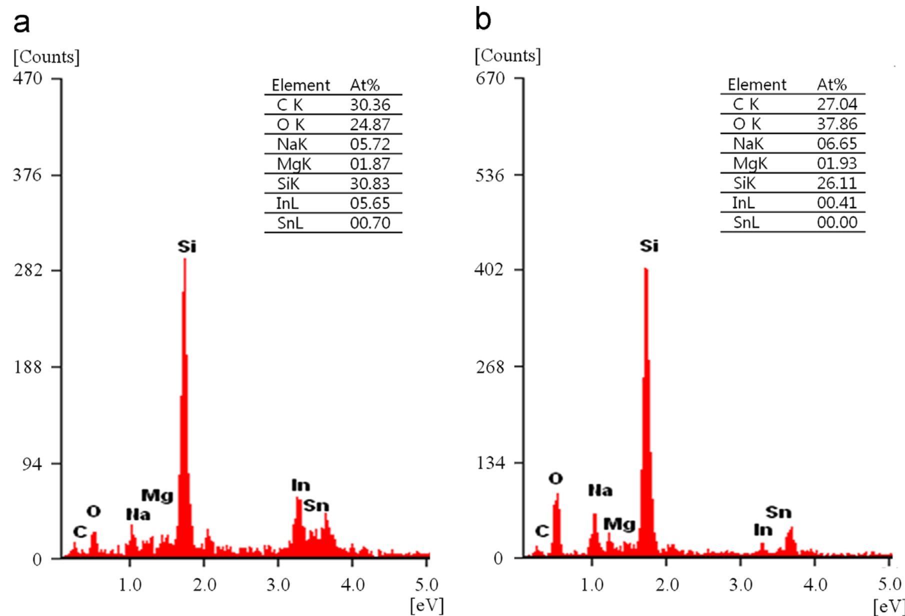

Fig. 6. Image of the EDS data atomic percent components: (a) before irradiation and (b) after irradiation with the six shots in Fig. 5(f).

pulse energy to get the finest depth control should be studied in future. With regard to the influence of the direction of polarization on ITO thin film and its ablation rate, the single pulse process is not likely to have a significant effect. However, to obtain accurate ablation rate with the proper polarization, further study is required on the influence of the ITO thin film, scan direction and proper polarization.

An energy dispersive spectrometer (EDS) was used to investigate the remained elements at the ablated area before and after the laser ablation because a visual contrast of the optical microscopic information did not reveal the chemical composition change. The results were presented in Fig. 6. In order to evaluate whether the selective ablation was achieved or not after the laser irradiation of six pulses (Fig. 5(f)), the residual percentages of indium and tin based ITO thin film was measured. The atomic percent (at%) of each element through peak fitting was presented in Fig. 6. The atomic percent of indium (In) and tin (Sn) were clearly decreased in the ablated area after six pulses of laser irradiation. The ITO was primarily composed of Sn and In [18]. For Sn, the atomic percent changed from 0.7 at% to 0 at% after the ablation. Furthermore, for In, the atomic percent changed from 5.65 at% to 0.41 at% after the ablation. It was thought that the selective ablation of the ITO thin film occurred from the glass substrate. Therefore, it was proposed that the small amount of In that remained after the ablation came from the remaining debris in the ablated area. Thus, it was considered that the ITO layer on the glass substrate was selectively removed without damage to the glass.

As seen in Fig. 7, several sizes of ablations with square and rectangular shapes were demonstrated on the ITO thin film using single shot irradiation with a fluence of 0.8 J/cm^2, a pulse duration of 190 fs, and a wavelength of 1030 nm. The ablation depth was 40 nm in all ablation patterns. The ablation shapes were controlled the varying the *x*–*y* axis slit.

The stereo structure of the ablation was also demonstrated through varying the slit size at the single shot irradiation with a fluence of 0.8 J/cm^2, a pulse duration of 190 fs, and a wavelength of 1030 nm; this is seen in Fig. 8. The size of the patterned structure varied from 25×25 (μm) to 5×5 (μm) with square shapes as a result of controlling the single pulse number and slit size. The depth of each ablated layer was observed approximately 40 nm. The cross section of the stereo structure was depicted in Fig. 8(b).

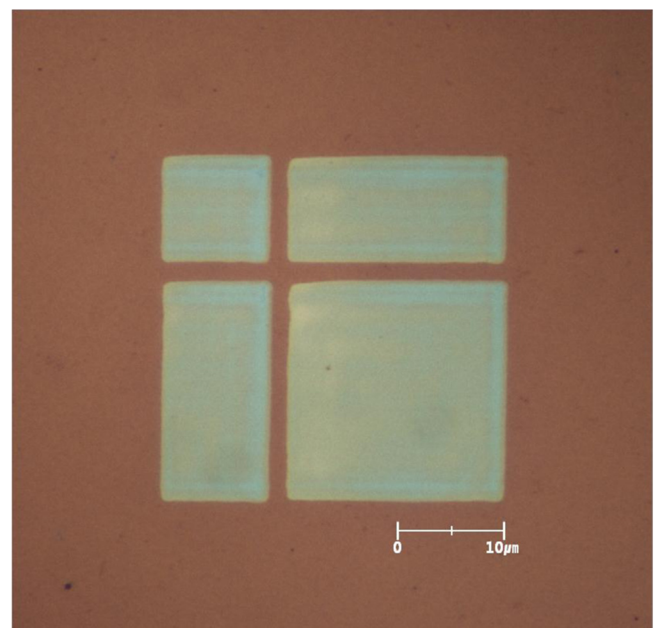

Fig. 7. Optical microscope views of the ablated rectangular and square shapes on the ITO thin film using the single pulse irradiation of the IR femtosecond laser. The ablation depth of the rectangular and square shapes was 40 nm.

The ablation depth was 40 nm at a size of 25×25 μm. However, the rate of ablated depth gradually decreased as the slit size decreased. When the last single pulse with a slit size of 5×5 was irradiated to structure the stereo shape, the shape of the cross section at the bottom of the ablated area almost reached flatness. The resolution of AFM at this situation was 0.001 nm. Considering the thickness of the ITO film and the ablation experiment with the pulse number control technique, this quantitatively explains that the ITO film was completely removed.

In this experiment, we demonstrated the depth control of ablation with a 40 nm resolution on an ITO thin film using square, flat beam shaped femtosecond lasers. The slit was used to make several types of flat beam shaped from the circular Gaussian beam. The fluence of the femtosecond laser irradiated on the surface of

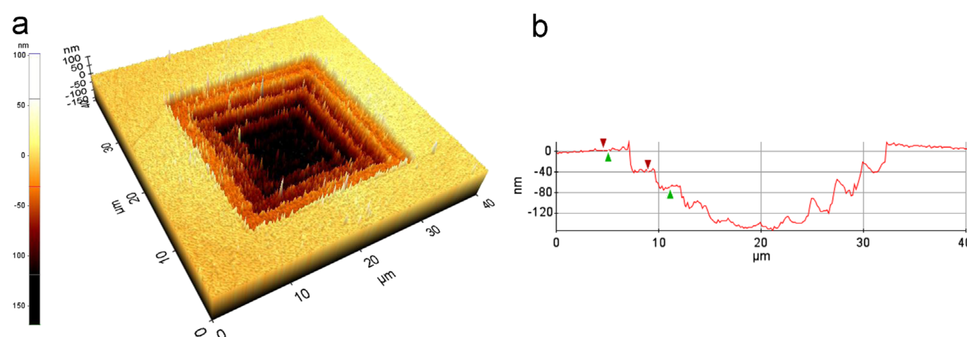

Fig. 8. Images of the (a) 3D stereo ablation and (b) cross-section morphology obtained from an AFM.

the ITO thin film was fixed at 0.8 J/cm^2 in order to investigate the depth control. The fluence was higher than the ablation threshold of the ITO thin film (0.14 J/cm^2) and less than the ablation threshold of the glass substrate (2.2 J/cm^2). Several research groups have reported investigations on ITO thin films [4], and ablation structures with slits have been reported in several papers applied in optical waveguides [19], solar cells [15], and electrical devices [6]. However, experimental results have not been demonstrated for well-defined shaped ablation structures on ITO thin films with the depth control of a 40 nm resolution using the NIR femtosecond laser. A high flatness ablation structure with well-defined square and rectangular shapes on the ITO thin film was fabricated on the surface of the ITO thin film. The obtained surface flatness in the ablated area was found less than 10 nm in this experiment.

Although several studies on ITO using nanosecond and picosecond lasers with ultra-violet (UV) wavelengths have been done, experimental results have not yet been reported on micromachining using femtosecond lasers in the UV wavelength, to the best of our knowledge. Based on the experimental results with nanosecond lasers [4,22] and picosecond lasers [23] in the UV wavelength range, it is expected that further improved depth control and more precise, fine processing can be achieved using a femtosecond laser in the UV wavelength due to the enhanced absorption.

From the analysis of the ablated surface morphologies with respect to the removal quality, it was found that the beam shaped NIR femtosecond laser with a slit was preferable for high surface flatness, fine edge ablated structures in comparison with a circular Gaussian beam [20]. Furthermore, it was considered that more precise pattern structures of optoelectronic devices could be achieved through using greater fine depth control. In addition, optoelectronic devices have strict specifications of high accuracy ITO processing with fine structures; in particular, well-defined edges are required [7].

The high height ridges of the ablated edges can frequently induce very critical contact problems in the organic manufacturing process of transparent conducting electrodes because organic electronic devices are composed of high-density multilayer thin film structures [21]. The thickness of the active films in optoelectronic devices is typically in the range of 100 nm [20]. The ridges at the ablated edges can cause short circuits in devices such as OLEDs and solar cells, or they can cause reductions in the working longevity and efficiency of the devices. Ashikenasi et al. reported that the minimum ridge height of an ablated area on an ITO film was more than 20 nm using Gaussian femtosecond lasers [17]. Thus, it is considered that the lower ridge height of 10 nm in the ablated area that was obtained in this experiment provides a significant advantage for the ITO ablation processing in optoelectronic devices. Furthermore, proper polarization control results in better ridge quality. The correlation between ridge quality and the scan direction, specific beam shape, and proper polarization need to be further studied to improve the ridge performance in the future.

4. Conclusion

In summary, ablation depth control with a resolution of 40 nm on ITO thin films was investigated with a pulse duration of 190 fs and a central wavelength of 1030 nm. A single pulse controlled square shaped femtosecond laser beam was used with a slit at the peak intensity of 2.8 TW/cm2. For the pulse shots from 1 to 6, the ablation depth ranged from 40 to 150 nm. The slit was used to create several types of flat top beam shapes with squares and rectangles from the Gaussian spatial beam profile of the femtosecond laser. When 6 pulses were irradiated, the atomic percent changed from 0.7 at% to 0 at% for Tin and from 5.65 at% to 0.41 at% for Indium after the ablation was achieved with EDS. The results of this study could be useful in the precision machining design of maskless procedures to control the ablation depth of ITO thin films on glass substrates in the field of optoelectronic devices, such as mobile phones, OLEDs, solar cells, and touch panels.

Acknowledgment

This work was partially supported by the Center for Advanced Meta-Materials(CAMM) (No. 2014M3A6B3063707) funded by the Ministry of Science, ICT and Future Planning as Global Frontier Project (CAMM- No. 2014M3A6B3063707).

References

[1] Afshar M, Straub M, Voellm H, Feili D, Koenig K, Seidel H. Sub-100 nm structuring of indium-tin-oxide thin films by sub-15 femtosecond pulsed near-infrared laser light. Opt Lett 2012;37:563–5.
[2] Cheng CW, Shen WC, Lin CY, Lee YJ, Chen JS. Fabrication of micro/nano crystalline ITO structures by femtosecond laser pulses. Appl Phys A 2010;101:243–8.
[3] Hoheisel M, Mitwalsky A, Mrotzek C. Microstructure and etching properties of sputtered indium-tin oxide (ITO). Phys Stat Sol 1991;123:461–72.
[4] Chen MF, Hsiao WT, Ho YS, Tseng SF, Chen YP. Laser patterning with beam shaping on indium tin oxide thin films of glass/plastic substrate. Thin Solid Films 2009;518:1072–8.
[5] Lee S, Yang D, Nikumb S. Femtosecond laser patterning of Ta0.1W0.9Ox/ITO thin film stack. Appl Surf Sci 2007;253:4740–7.
[6] Li ZH, Cho ES, Kwon SJ. A new laser direct etching method of indium tin oxide electrode for application to alternative current plasma display panel. Appl Surf Sci 2009;255:9843–6.
[7] Raciukaitis G, Brikas M, Gedvilas M, Darcianovas G. Patterning of ITO layer on glass with high repetition rate picoseconds lasers. J Laser Micro Nanoeng 2007;2:1–6.
[8] Choi HW, Farson DF, Bovatsek J, Arai A, Ashkenasi D. Direct-write patterning of indium-tin-oxide film by high pulse repetition frequency femtosecond laser ablation. Appl Opt 2007;46:5792–9.

[9] Park M, Chon BH, Kim HS, Jeoung SC, Kim D, Lee JI, et al. Ultrafast laser ablation of indium tin oxide thin films for organic light-emitting diode application. Opt Laser Eng 2006;44:138–46.
[10] Cavallo P, Rodriguez RC, Broglia M, Acevedo DF, Barbero CA. Simple fabrication of active electrodes using direct laser transference. Electrochim Acta 2014;116:194–202.
[11] Fitzsimons PW, Kuang Z, Perrie W, Edwardson S, Dearden G. Parallel patterning of indium tin oxide with ultra-short pulses. Surf Eng 2013;29:660–6.
[12] Xu MY, Li J, Lilge LD, Herman PR. F2-laser patterning of indium tin oxide (ITO) thin film on glass substrate. Appl Phys A 2006;85:7–10.
[13] Cheng CW, Lin CY. High precision patterning of ITO using femtosecond laser annealing process. Appl Surf Sci 2014;314:215–20.
[14] Kwon SJ. Patterning properties of indium-tin oxide layer depending on the irradiation conditions of Nd:YVO_4 laser beam. J Appl Phys 2008;47:7403–6.
[15] Bian Q, Yu X, Zhao B, Chang Z, Lei S. Femtosecond laser ablation of indium tin-oxide narrow grooves for thin film solar cells. Opt Laser Tech 2013;45:395–401.
[16] Kim HJ, Seo KW, Kim YH, Choi J, Kim HK. Direct laser patterning of transparent ITO-ag-ITO multilayer anodes for organic solar cells. Appl Surf Sci 2015;328:215–21.
[17] Ashkenasi D, Muller G, Rosenfeld A, Stoian R, Hertel IV, Bulgakova NM, et al. Fundamentals and advantages of ultrafast micro-structuring of transparent materials. Appl Phys A 2003;77:223–8.
[18] Rung S, Christiansen A, Hellmann R. Influence of film thickness on laser ablation threshold of transparent conducting oxide thin-films. Appl Surf Sci 2014;305:347–51.
[19] Luff BJ, Wilkinson JS, Perrone G. Indium tin oxide over layered waveguides for sensor applications. Appl Opt 1997;36:7066–72.
[20] Yavas O, Takai M. Effect of substrate absorption on the efficiency of laser patterning of indium tin oxide thin films. J Appl Phys 1999;85:4207–12.
[21] Xuefei S, Tao C, Ning L. Patterning of ITO on glass with two-step using excimer laser and wet chemical re-etching. Adv Mater Res 2011;8:291–4.
[22] Rung S, Rexhepi M, Bischoff C, Hellmann R. Laserscribing of thin films using top-hat laser beam profiles. J Laser Micro/Nanoeng 2013;8:309–14.
[23] Raciukaitis G, Brikas M, Gedvilas M, Rakickas T. Patterning of indium-tin oxide on glass with picosecond lasers. Appl Surf Sci 2007;253:6570–4.